



HAL
open science

Impact of Polyethylenimine Conjugation Mode on the Cell Transfection Efficiency of Silica Nanovectors

Xiaolin Wang, Sylvie Masse, Guillaume Laurent, Christophe Hélyary, T. Coradin

► **To cite this version:**

Xiaolin Wang, Sylvie Masse, Guillaume Laurent, Christophe Hélyary, T. Coradin. Impact of Polyethylenimine Conjugation Mode on the Cell Transfection Efficiency of Silica Nanovectors. *Langmuir*, 2015, 31 (40), pp.11078-11085. 10.1021/acs.langmuir.5b02616 . hal-01274327

HAL Id: hal-01274327

<https://hal.science/hal-01274327>

Submitted on 1 Oct 2018

HAL is a multi-disciplinary open access archive for the deposit and dissemination of scientific research documents, whether they are published or not. The documents may come from teaching and research institutions in France or abroad, or from public or private research centers.

L'archive ouverte pluridisciplinaire **HAL**, est destinée au dépôt et à la diffusion de documents scientifiques de niveau recherche, publiés ou non, émanant des établissements d'enseignement et de recherche français ou étrangers, des laboratoires publics ou privés.

Impact of Polyethyleneimine Conjugation Mode on the Cell Transfection Efficiency of Silica Nanovectors

Xiaolin Wang, Sylvie Masse, Guillaume Laurent, Christophe H elary,* and Thibaud Coradin*

Sorbonne Universit es, UPMC Univ Paris 06, CNRS, UMR 7574, Laboratoire de Chimie de la Mati re Condens e de Paris, F-75005 Paris, France

ABSTRACT: The conjugation of polyethyleneimine (PEI) to silica nanoparticles has emerged as a useful strategy in gene delivery. Here we investigate the influence of the PEI conjugation mode on the transfection ability of plain silica nanoparticles. Surface functionalization with sulfonate- and chloride-bearing silanes modulates the amount and conformation of PEI, and therefore the particles' affinity for the plasmid, without impacting on cytotoxicity. However, transfection efficiency in both immortalized and primary cells is more directly correlated to the nature and strength of the particle-PEI interactions. It suggests that PEI detachment from the particle surface at the stage of endosomal escape is a key event in the plasmid delivery process. These data should provide fruitful guidelines for the fine tuning of colloidal surfaces intended for intracellular delivery of bioactive molecules.

INTRODUCTION

Gene therapy is considered as a breakthrough in regenerative medicine as it permits to correct genetic disorders.^{1,2} More recently, gene delivery strategies have been used to modulate impaired gene expressions observed in chronic diseases.^{3,4} In this case, therapeutic genes do not need to be inserted in the genome but are transitory expressed. Therapeutic genes can take the form of shRNA, siRNA or plasmidic DNA.⁵⁻⁷ Because of their negative charge, nucleic acids are unable to penetrate into the cells. As a consequence, they need to be combined with a transfecting reagent to penetrate the mammalian cells. Viral vectors are broadly used as they present the highest transfection efficiencies.⁸ Nonetheless, these systems have several limitations such as their immunogenicity and oncogenicity.⁹ These drawbacks justified the development of non-viral vectors such polymeric transfecting reagents.⁹ PEI has been deemed as one of the most efficient polymeric transgene reagent in virtue of the 'proton sponge effect', that enables endosomal escape and translocation of DNA into the nucleus.¹⁰ However, the cytotoxicity accompanying high transfection efficiency greatly impairs its clinical

1
2
3
4 applications. Efforts have been devoted to find a compromise between the two
5
6 phenomena, by chemical modification of PEI or its conjugation to nanoparticles.¹¹
7
8

9
10 Nanoscale delivery systems hold great promise for gene therapy owing to their ability
11
12 to enhance cellular uptake and intracellular stability of nucleic acids.¹² For gene delivery,
13
14 the generation of positive charges on the particle external or internal surface is required to
15
16 complex negatively-charged nucleic acids. A common solution is to modify nanoparticle
17
18 surface with amino-alkoxysilane³ or cationic polymers,¹³⁻¹⁶ among which
19
20 polyethyleneimine (PEI) has drawn considerable interest. The combination of particles
21
22 with PEI was first studied to promote polyplex transfection efficiency, in which
23
24 nanoparticles was applied to enhance sedimentation of polyplexes at cell surface. Silica
25
26 nanoparticles have emerged as ideal candidates due to their biocompatibility, facile
27
28 fabrication, tunable size/porosity and easy surface functionalization.¹⁷ Silica
29
30 nanoparticles were first studied as drug delivery systems to target tumoral cells or to
31
32 deliver antibiotics inside the cells.^{18,19} For example, several studies have shown the
33
34 delivery of high doses of doxorubicin within multi-resistant cancer cells.²⁰ SiO₂-PEI
35
36 particles have emerged as versatile drug/gene vehicles that can be synthesized by *in situ*
37
38 polymerization,²¹ electrostatic adsorption²² and covalent bonding.²³ However the impact
39
40 of the PEI bioconjugation mode to silica particles on its conformation and on the carrier
41
42 transfection efficiency has not been examined so far.
43
44
45
46
47
48
49
50
51
52
53
54

55 To address this question, we have compared here three methods to conjugate PEI with
56
57 plain silica nanoparticles, from non-specific electrostatic interactions to covalent bonding
58
59
60

(Figure 1). We show that the mode of conjugation impacts on the amount and conformation of immobilized PEI and that the transfection efficiency is directly related to the nature of the particle-PEI interactions, both in immortalized fibroblasts and primary keratinocytes. These results have important implications for the design of nanovectors for intracellular drug delivery.

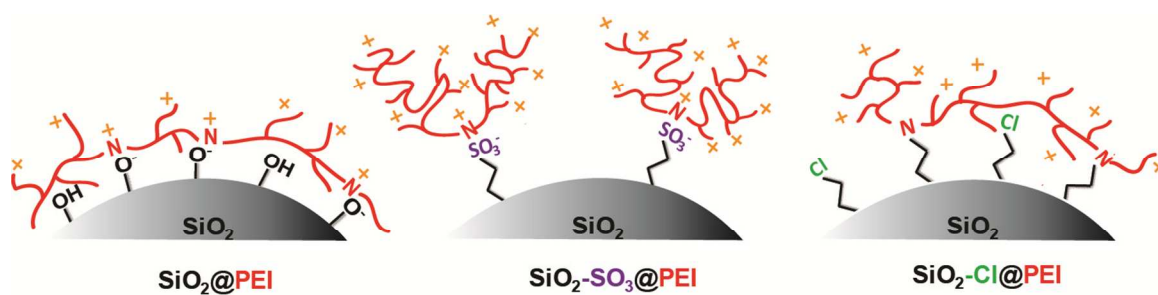


Figure 1. Schematic representation of the different conjugation modes of polyethyleneimine (PEI) with silica particles and proposed PEI configuration: non-specific adsorption on silica particles ($\text{SiO}_2\text{@PEI}$), strong electrostatic interactions with sulfonate-modified silica particles ($\text{SiO}_2\text{-SO}_3\text{@PEI}$) and covalent bond with propylchloride-grafted silica particles ($\text{SiO}_2\text{-Cl@PEI}$).

MATERIALS AND METHODS

Silica-polyethyleneimine particle preparation. Silica nanoparticles SiO_2 were synthesized by the Stöber method²⁴ using 7.6 mL of tetraethylorthosilicate (TEOS), 200 mL of ethanol, 9.7 mL of ammonia (25 %) and 5.9 mL of deionized water. For $\text{SiO}_2\text{@PEI}$ particle preparation, 200 mg of branched polyethyleneimine PEI (25 kDa) was

1
2
3
4 dissolved in 20 mL of saline phosphate buffered saline (PBS, 10 mM, pH 7.4).²⁵ Silica
5
6 nanoparticle suspension in PBS (20 mL) was then added dropwise into the PEI solution
7
8 under stirring. The mixtures were stirred for 48 h after which particles were recovered by
9
10 centrifugation, washed 3 times in PBS and finally suspended in PBS.
11
12
13

14
15 For SiO₂-SO₃@PEI particle preparation, the SiNP was first functionalized with thiol
16
17 groups by silylation with 3-mercaptopropyltrimethoxysilane (MPTMS).²⁶ Typically, 1 g
18
19 of silica was dispersed in a mixture of 100 mL ethanol and 2.2 mL ammonium hydroxide
20
21 solution before addition of 1 mL MPTMS. The mixture was stirred for 40 min at room
22
23 temperature. Subsequently, the reaction mixture was heated to 80 °C and the total volume
24
25 was reduced by 2/3 by distillation of ethanol and ammonia at ambient pressure. Then, the
26
27 mixture was cooled back to room temperature, centrifuged, washed 3 times with ethanol
28
29 and dried at 60 °C. Then 0.9 g of the thus-obtained SiO₂-SH was suspended in 45 mL
30
31 hydrogen peroxide (H₂O₂ 35%, Acros Organics) under stirring at room temperature for
32
33 48 hours. The solid product was washed by centrifugation with distilled water before
34
35 addition of 35 mL of concentrated sulfuric acid (H₂SO₄ 95.0-98.0%, Sigma Aldrich) and
36
37 stirred for 2 hours. Finally the as-synthesized SiO₂-SO₃ particles were washed with water,
38
39 suspended in PBS and coated with PEI as described above.
40
41
42
43
44
45
46
47
48
49

50
51 For SiO₂-Cl@PEI particle preparation, 400 mg of SiO₂ nanoparticles was dispersed
52
53 in 20 mL of dried toluene, and 1.3 mL of chloropropyltriethoxysilane (Cl-PTES) was
54
55 added to the suspension, that was further kept under reflux for 24 h, after which the
56
57
58
59
60

1
2
3
4 product was washed thoroughly with toluene and ethanol, and dried at room temperature.
5
6
7 Then, 200 mg SiO₂-Cl was dispersed in 20 mL ethanol, and 0.8 g of PEI was added to the
8
9
10 suspension. The suspension was refluxed for 24 h. The final solid product was recovered
11
12 by washing with ethanol and dried at room temperature. The as-synthesized
13
14 SiNP-Cl@PEI was suspended in 10 mM PBS before use.
15
16

17
18 **Silica-polyethyleneimine particle characterization.** Sizes and zeta potential (ζ)
19
20 were measured in 10 mM PBS solution using a ZetaSizer Nano (Malvern Instruments
21
22 Ltd., Worcestershire, UK). Particles were also imaged using Transmission Electron
23
24 Microscopy (TEM) on a JEOL 1011 instrument. The amount of adsorbed PEI was
25
26 determined by elemental analysis (C,H,O,N). For SiO₂-SO₃, the grafting rate was
27
28 calculated according to the amount of -SH before oxidation, which is determined by
29
30 Ellman test.²⁷ For this test, a phosphate buffer (0.2 M, pH = 7.3) was prepared and
31
32 labeled as solution A. Solution B (10 mM EDTA) was produced by dissolving 372 mg of
33
34 EDTA in 100 mL of solution A, and solution C (6 mM
35
36 5-(3-Carboxy-4-nitrophenyl)disulfanyl-2-nitrobenzoic acid (DTNB)) was prepared by
37
38 dissolving 238 mg of DTNB in 100 mL of solution A. Several vials were filled with a
39
40 mixture of 8 ml of solution A, 1 mL of solution B and 1 mL of solution C. A series of
41
42 masses of SiO₂-SH, less than 50 mg, were measured and then each dispersed into a vial
43
44 mixture solution. Simultaneously, several known quantities of thiol (obtained from a
45
46 solution of MPTMS) were also introduced in the same mixture solution to determine the
47
48
49
50
51
52
53
54
55
56
57
58
59
60

1
2
3
4 molar extinction coefficient by linear regression. After 45 minutes of stirring, the particle
5
6 dispersion is filtered through a syringe filter. The absorbance of the filtrate and standard
7
8 MPTMS solutions are determined by spectroscopy. The absorbance of the solutions
9
10 MTPMS can be traced back to the value for the experience of the molar extinction
11
12 coefficient of NTB²⁻ by linear regression.
13
14
15
16
17

18
19 XPS analyses of the powders were performed on a Phoibos 100 X-ray photoelectron
20
21 spectrometer (SPECS GmbH, Germany) with the Mg K α X-ray source (h ν =1253.6 eV).
22
23 Spectra were recorded with 20 eV pass energy for the survey scan and with 10 eV pass
24
25 energy for the C 1s, O 1s, N 1s, S 2s and Si 2p regions. A take-off angle of 90° from the
26
27 surface was employed. Element peak intensities were corrected by Scofield factors and
28
29 the spectra were fitted using the Casa XPS v.2.3.13 Software (Casa software Ltd. UK)
30
31 and by applying a Gaussian/Lorentzian ratio, G/L equal to 70/30.
32
33
34
35
36
37

38 **pDNA-PEI and pDNA-PEI-SiNP Complexation.** Reporter plasmid pCMV-GLuc
39
40 (pGluc) encoding for Gaussia Luciferase (New England BioLabs, Ipswich, MA) was
41
42 used to quantify transgene expression. This plasmid was amplified by one shot[®]
43
44 BL21(DE3) pLysS kit (Invitrogen[™], Life technologies), extracted by one PureLink[®]
45
46 HiPure Plasmid kit (Invitrogen[™], Life technologies) and finally stored in Tris-EDTA
47
48 buffer at -20 °C. pGluc-PEI complexes were prepared at weight ratio of 1:2. pGluc-
49
50 SiO₂-X@PEI (X = none, SO₃, Cl) complexes were prepared at various weight ratios.
51
52
53
54
55
56
57 Complexes formation was examined by agarose gel electrophoresis. Briefly, 1 μ L of
58
59
60

1
2
3
4 pGluc solution ($0.1 \mu\text{g} \cdot \mu\text{L}^{-1}$) were mixed homogeneously with a total volume of $9 \mu\text{L}$ of
5
6
7 $\text{SiO}_2\text{-X@PEI}$ suspension or PEI solution (PBS 1x) by vortexing in a microcentrifuge
8
9
10 tube. The resulting mixtures were left at room temperature for 2 h to achieve complete
11
12 complexation, before being loaded onto 0.7% agarose gel with ethidium bromide (0.1
13
14 $\mu\text{g} \cdot \text{mL}^{-1}$) and running with TAE buffer at 100 V for 40 min. DNA retardation was
15
16
17 observed by irradiation with ultraviolet light.
18
19

20
21 **Cell Transfection and Cell Viability.** 3T3 mouse fibroblasts were cultured in
22
23 complete cell culture medium (Dulbecco's Modified Eagle's Medium (DMEM)
24
25 supplemented with 10% fetal serum, $100 \text{ U} \cdot \text{mL}^{-1}$ penicillin, $100 \mu\text{g} \cdot \text{mL}^{-1}$ streptomycin
26
27 and $0.25 \mu\text{g} \cdot \text{mL}^{-1}$ Fungizone). Primary normal human keratinocytes (NHK) were cultured
28
29 in keratinocytes growth medium 2 (Promocell) supplemented with CaCl_2 . Tissue culture
30
31
32 flasks (75 cm^2) were kept at $37 \text{ }^\circ\text{C}$ in a 95 % air: 5 % CO_2 atmosphere. Before
33
34
35 confluence, cells were removed from culture flasks by treatment with 0.1% trypsin and
36
37
38 0.02 % EDTA. Cells were rinsed and suspended in the appropriate culture medium before
39
40
41 use.
42
43
44

45
46 Transfection efficiency of pGluc-PEI and pGluc- $\text{SiO}_2\text{-X@PEI}$ were evaluated by
47
48 luciferase expression of pGLuc by cells in cell culture medium. To perform cell
49
50 transfection, mouse fibroblasts or human keratinocytes were plated at a density of $5 \cdot 10^4$
51
52
53 per well in a 24-well plate. pGluc-PEI or pGluc- $\text{SiO}_2\text{-X@PEI}$ complexes ($25 \mu\text{L}$) were
54
55
56 added to the cell culture medium. After 4 h, the supernatant was removed, the well was
57
58
59
60

1
2
3
4 refreshed with 1 mL medium and the cells were then cultured for another 44 h in
5
6 complete medium for the expression of luciferase. For measurements of luciferase
7
8 activity, a BioLux Gaussia Luciferase Assay Kit (New England Biolabs) was used and
9
10 transgene expression of luciferase was reported as relative light units (RLU). Control
11
12 groups were under the same culture condition as the experiment groups except for the
13
14 absence of DNA complexes.
15
16
17
18

19
20 Internalization of nanoparticles in 3T3 mouse fibroblasts was studied using
21
22 fluorescence microscopy. Fluorescent silica particles 200 nm in diameter were prepared
23
24 according to a previously described protocol²⁸ and modified according to the
25
26 above-described procedure. The pGluc-fluorescent nanoparticles complexes along with
27
28 cell culture medium were removed after a 24 h incubation period, rinsed 3 times with
29
30 PBS and fixed with 4% paraformaldehyde for 1 hour at room temperature. The cell
31
32 nucleus was then stained with DAPI (4',6-diamidino-2-phenylindole dihydrochloride,
33
34 Life technologies, 300 nM in PBS) for 10 min and rinsed with PBS before observation.
35
36
37
38

39
40 Cell viability was monitored using the Alamar Blue test. For the 2D model, cell
41
42 culture medium was removed for luciferase activity test and 200 μ L of the Alamar Blue
43
44 solution (10% in cell culture medium) was added. The cells were then incubated at 37 $^{\circ}$ C
45
46 with 5 % CO₂ for 4 h. The supernatant in each well was then collected, diluted with 800
47
48 μ L water, and its absorbance was measured at $\lambda = 570$ nm and 600 nm. Cell viability was
49
50 calculated and reported as a percentage of the control group (n = 6).
51
52
53
54
55
56
57
58
59
60

RESULTS AND DISCUSSION

Chemical properties of PEI-coated silica nanoparticles. Silica nanoparticles SiO₂ were synthesized by the Stöber method and obtained with a low size dispersity (210 ± 20 nm, from TEM with a polydispersity index PDI = 0.005) (**Figure S1**). After coating with PEI, the particle hydrodynamic diameter (d) in PBS was not significantly modified but the PDI significantly increased to 0.127. The zeta potential (ζ) value turned from negative to positive in PBS, in agreement with the deposition of a cationic polymer (**Table 1**). In the case of sulfonated SiO₂-SO₃ particles, neither surface functionalization nor PEI sorption significantly impacted on the colloidal size distribution. The mean ζ value of SiO₂-SO₃ particles was slightly more negative than for bare silica, due to the presence of acidic sulfonate moieties, but the ζ value after PEI coating was similar for both particles. The SiO₂-Cl nanoparticles showed a high tendency to aggregate, as such and after PEI conjugation, with high PDIs in both situations. However, the ζ values were not significantly different from the two previous systems (**Table 1**).

Elemental analysis allowed for quantification of grafted moieties and amount of surface PEI (**Table 1**). For SiO₂-SO₃, the S content was below 0.1 wt% so that the silane density was obtained by the Ellman test, yielding to *ca.* 1.5×10^4 groups per particle. For SiO₂-Cl, grafting density was estimated to *ca.* 1.5×10^6 silanes per particle. Upon reaction with PEI, the Cl:Si ratio was decreased by half, supporting the occurrence of a nucleophilic substitution reaction between the propylchloride moieties and amine groups.

The extent of the alkylation reaction was qualitatively supported by ^{13}C NMR experiments evidencing a significant decrease of the mobility of the α C of the chloropropyl chain after reaction with PEI (**Figure S2**). The highest amount of bound PEI was obtained for $\text{SiO}_2@\text{PEI}$ (12 wt%) while the two other systems had a significantly lower binding capacity (4 wt% for $\text{SiO}_2\text{-SO}_3@\text{PEI}$ and 3 wt% for $\text{SiO}_2\text{-Cl}@\text{PEI}$).

Table 1. Hydrodynamic diameter (d) with polydispersity index (PDI), zeta potential (ζ) in PBS, elemental analysis and calculated composition of the particles.

	d (nm)	ζ (mV)	PDI	Cl:Si (wt%)	N:Si (wt%)	PEI (wt%)	silane/ particle	amine/ particle
SiO_2	214 ± 17	-15 ± 6	0.005	-	-	-	-	-
$\text{SiO}_2@\text{PEI}$	188 ± 68	$+20 \pm 7$	0.126	-	11.0	12.7	-	5×10^6
$\text{SiO}_2\text{-SO}_3$	233 ± 38	-21 ± 8	0.027	-	-	-	1.5×10^{4a}	-
$\text{SiO}_2\text{-SO}_3@\text{PEI}$	221 ± 20	$+21 \pm 9$	0.008	-	3.8	4.2	ND ^b	1.5×10^6
$\text{SiO}_2\text{-Cl}$	518 ± 308	-13 ± 6	0.314	2.7	-	-	1.7×10^6	-
$\text{SiO}_2\text{-Cl}@\text{PEI}$	806 ± 642	$+18 \pm 9$	0.635	1.1	3.1	3.4	ND ^b	10^6

^afrom Ellman titration; ^bND= not determined

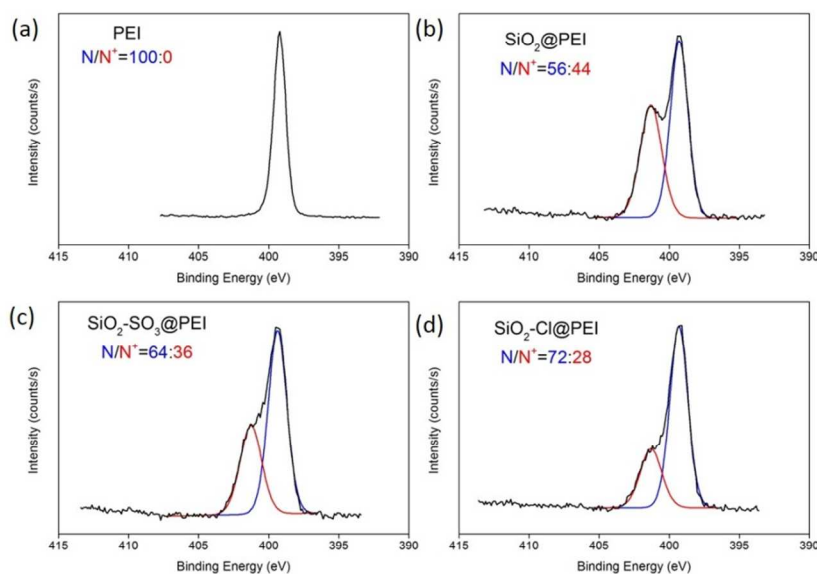


Figure 2: XPS spectra of (a) pure PEI, (b) SiO₂@PEI, (c) SiO₂-SO₃@PEI and (d) SiO₂-Cl@PEI at the N_{1s} level.

The surface composition of the particles was studied by X-ray Photoelectron Spectroscopy (XPS) (**Figure 2** and **Figure S3**). For PEI, carbon and nitrogen elements are identified in a C:N atomic ratio of 70:30, in fair agreement with the overall C₂H₅N formula of ethylene imine. The C_{1s} data show an asymmetric peak in the 284-288 eV region, corresponding to the overlap of C-C (285 eV) and C-N (287 eV) signals.²⁹ The N_{1s} signal consists of a single peak centered at 399 eV that can be attributed to primary/secondary/tertiary amines. For SiO₂, the typical peaks of amorphous silica are observed at 103 eV (Si_{2p}) and 534 eV (O_{1s}).³⁰ A weak C_{1s} signal is also obtained that can be attributed to carbon surface contamination as well as possible unhydrolyzed Si(OC₂H₅)

1
2
3
4 moieties. The XPS spectrum of SiO₂@PEI particles combines the Si, O and C peaks of
5
6 SiO₂ and PEI. However, the N_{1s} data showed two populations at 399 eV and 401 eV in a
7
8 56:44 intensity ratio, the latter corresponding quaternary amines (**Figure 2**).³¹ The
9
10 presence of sulfonate groups could be ascertained by the presence of a S_{2s} signal at 232 eV
11
12 for SiO₂-SO₃.³² Compared to SiO₂, the C_{1s} region showed an additional signal near 289 eV
13
14 that can be attributed to the C-S bond. PEI coating did not significantly modify the C, O,
15
16 Si and S signals. At the N_{1s} level, the 399 eV and 401 eV peaks are again identified but
17
18 with an intensity ratio of 64:36 (**Figure 2**). For SiO₂-Cl, the Cl_{2p} peak near 200 eV
19
20 confirms the successful grafting of Cl-PTES.³³ Similarly to SiO₂-SO₃, the C_{1s} signal shows
21
22 a high energy contribution corresponding to C-Cl bond. For SiO₂-Cl@PEI, the Cl_{2p} signal
23
24 was still clearly evidenced but a slight decrease of the Cl:Si ratio was found, in qualitative
25
26 agreement with the elemental analysis results. The signal at the N_{1s} level indicates a
27
28 unprotonated:protonated amine ratio of 72:28 (**Figure 2**), the highest value in this series.
29
30
31
32
33
34
35
36
37

38
39 Using the reporter plasmid pCMV-GLuc (pGluc), the optimal plasmid:particle ratio
40
41 was determined using gel electrophoresis (**Figure 3**). Full retention was achieved for
42
43 pG-Luc:SiO₂@PEI and pG-Luc:SiO₂-SO₃@PEI: weight ratios of 1:30 whereas a 1:50
44
45 ratio was optimal for pGLuc:SiO₂-Cl@PEI. As a comparison, the optimal pG-Luc:PEI
46
47 ratio was 1:2.
48
49
50
51
52
53
54
55
56
57
58
59
60

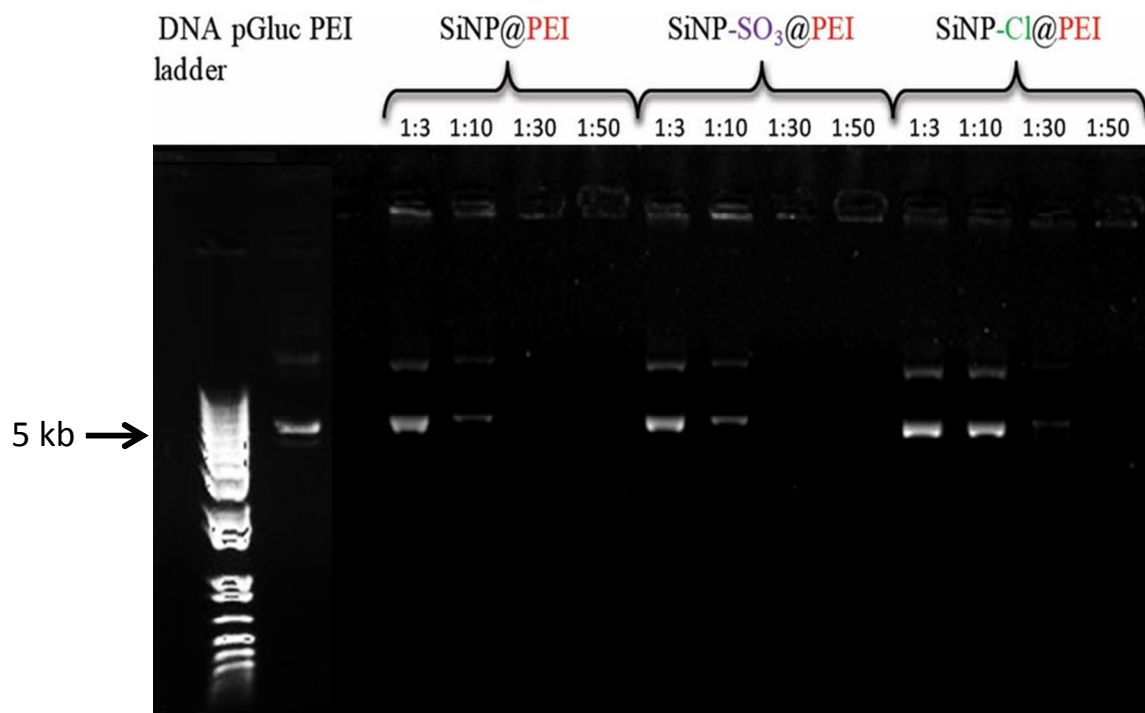


Figure 3: Agarose gel electrophoresis showing the influence of PEI conjugation mode on pGLuc complexation. A constant amount of pGLuc was complexed with particles at 1:3, 1:10, 1:30 and 1:50 weight ratios.

These data indicate that the conjugation mode impacts on PEI content, charge and plasmid binding ability. For $\text{SiO}_2\text{@PEI}$, using a particle radius of 100 nm and a silica density of $2 \text{ g}\cdot\text{cm}^{-3}$, the total amount of amine groups per particle can be estimated to *ca.* $5\cdot 10^6$ from elemental analysis (**Table 1**). The ammonium/total amine ratio obtained by XPS is *ca.* 45 % (*i.e.* *ca.* $2.2\cdot 10^6$ ammonium per particle). As a comparison a 30 % value was reported for PEI in a buffer solution (pH 7.4), suggesting that partial PEI protonation occurred during the adsorption process.³⁴ A density of 3-5 silanol per nm^2 was reported for amorphous silica surfaces, *i.e.* $4\text{-}6\cdot 10^5$ SiOH for 200 nm particles, with 20 % of acidic

1
2
3
4 (pKa = 4.5) and 80 % of basic (pKa = 8.5) groups.³⁵ The increase in PEI protonation may
5
6 therefore arise from an acid-base reaction with the silanol groups. Comparing 5×10^5 SiOH
7
8 with 2.2×10^6 N⁺ per particle, the silanol:ammonium ratio is 1:4-5 so that the positive
9
10 charge of PEI is not balanced by the negative charge of silica, explaining the positive ζ
11
12 value of these systems.
13
14
15

16
17 For SiO₂-SO₃@PEI, the protonation degree of PEI is closer to the reported value in
18
19 buffer (36 % vs. 30 %). Sulfonate groups are fully deprotonated at pH 7 so that proton
20
21 exchange with PEI was not expected. The fact that the silanol groups do not significantly
22
23 interact with the polymer suggests that PEI is kept apart from the silica surface.
24
25 Interestingly, combined elemental analysis and XPS indicate that there are 5×10^5
26
27 ammonium groups per particle to be compared with 1.5×10^4 sulfonate groups. This
28
29 observation can be compared with a recent study devoted to the sorption of collagen triple
30
31 helices on the surface of silica particles.²⁶ For bare particles, a large amount of collagen
32
33 was readily adsorbed, suggesting that the protein adopts a flat configuration on the particle
34
35 surface. In contrast, sulfonate-bearing particles could adsorb less collagen but the proteins
36
37 had a more ordered organization. It was suggested that the sulfonate groups could act as
38
39 anchoring points for the protein chains that protrude out of the surface rather than laying
40
41 flat, so that the amount of sorbed collagen was limited by the steric constraints of the triple
42
43 helices packing. A similar situation can be reasonable assumed for the present system
44
45
46
47
48
49
50
51
52
53
54
55 (**Figure 1**). Noticeably, naked particles have a lower initial negative charge, bind more
56
57 PEI with a higher degree of protonation than sulfonated ones, so that it was expected that
58
59
60

1
2
3
4 they exhibit a higher positive surface charge after coating. However the two systems show
5
6 close ζ values. This can be explained considering that silanol groups of the surface can
7
8 contribute to the overall particle charge for SiO₂ whereas these moieties are screened by
9
10 the sulfonate/PEI layer, strengthening our model of a flat vs. compact organization of the
11
12 polymer in the two systems.
13
14
15

16
17 For SiO₂-Cl@PEI, the protonation degree of PEI is similar to its free form in buffer
18
19 and the number of amines per particle is *ca.* 10⁶. This value is in the same range as the
20
21 initial density of propylchloride groups (1.5x10⁶). Elemental analysis indicate that one half
22
23 of the Cl atoms are no longer present after reaction with PEI. Taken together these data
24
25 suggest that an important fraction of the PEI amine groups have reacted with the
26
27 propylchloride moieties. It is therefore possible to assume that each PEI chain is bound to
28
29 the particle surface by several anchoring points, decreasing its conformational flexibility
30
31 and therefore its maximum packing density on the surface, resulting in a low PEI loading
32
33 (**Figure 1**). Noticeably, SiO₂-Cl@PEI has a similar ζ value to SiO₂@PEI, which can be
34
35 explained considering that the less negative surface charge of the chlorinated surface
36
37 compared to bare particles is compensated by lower PEI loading and lower PEI
38
39 protonation.
40
41
42
43
44
45
46
47
48

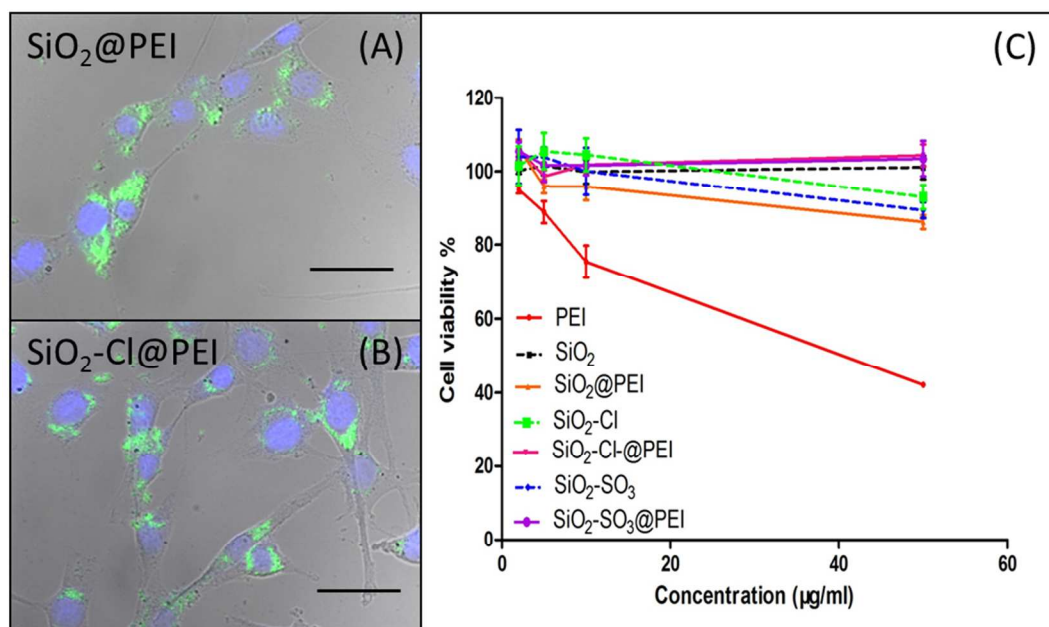
49 Considering the optimal plasmid:PEI ratio, it depends on the positive charge of PEI, as
50
51 the PEI-plasmid system is a polyelectrolyte complex, as well as on the PEI flexibility, that
52
53 determines its ability to wrap and compact DNA.^{10,36} The amount of PEI per particle must
54
55 also be considered for the optimal plasmid:particle ratio. SiO₂@PEI and SiO₂-SO₃@PEI
56
57
58
59
60

1
2
3
4 particles have a similar optimal pGLuc:particle@PEI ratio although the former has a
5
6 higher polymer loading with a larger proportion of ammonium groups than the latter. As
7
8 pointed out earlier, the ζ value is not a suitable parameter to compare the complexing
9
10 ability of the systems as it can include a contribution of the silica particle surface that is
11
12 not involved in the DNA wrapping process. Rather PEI conformation has to be considered
13
14
15
16
17 **(Figure 1)**. For SiO₂, the extended conformation of the polyelectrolyte is not favorable for
18
19 DNA wrapping whereas the local anchoring of PEI on the surface of Si-SO₃ should better
20
21 preserve its structural flexibility. For SiO₂-Cl, as mentioned earlier, its flexibility should be
22
23 limited by the high density of covalent bonds, resulting in a low pG-Luc:particle@PEI
24
25
26
27
28 ratio.
29
30
31
32

33 **Biological properties of PEI-coated silica nanoparticles.**

34
35
36 Delivery of therapeutic genes from PEI-coated silica nanoparticles requires the
37
38 particles uptake by cells. Particle internalization within mouse 3T3 fibroblasts was
39
40 checked using fluorescent FITC-silica nanoparticles after 48 h of contact. Observations
41
42 by fluorescence microscopy evidenced the accumulation of colloids near the cell nucleus
43
44 for SiO₂@PEI and SiO₂-Cl@PEI **(Figure 4A)**. Bleaching of the FITC probes during
45
46 sulfonate particle preparation hindered their intracellular observation. Cytotoxicity of
47
48 uncoated and PEI-coated particles was also studied on 3T3 fibroblasts. This study
49
50 consisted in the measure of cell viability of fibroblasts incubated with increasing doses of
51
52
53
54
55
56
57
58 particles **(Figure 4B)**. For particle@PEI systems, cell viability was always higher than 80
59
60

1
2
3
4 %, indicating the absence of significant cytotoxicity up to $50 \mu\text{g}\cdot\text{mL}^{-1}$ in PEI. In contrast,
5
6
7 PEI alone was detrimental to cell viability at a dose $> 5 \mu\text{g}\cdot\text{mL}^{-1}$. Uncoated particles were
8
9
10 evaluated using the same silica weights, showing no visible cytotoxicity effect.

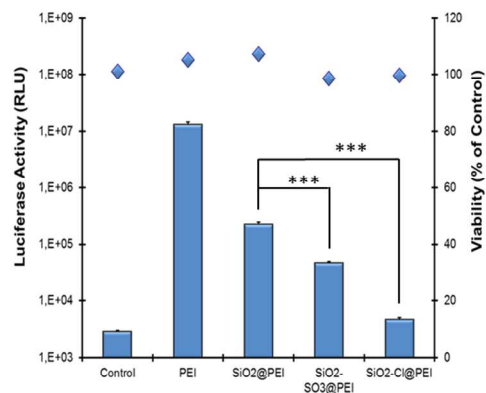


32
33
34
35
36 **Figure 4:** (A and B) Fluorescence microscopy image showing internalization of
37
38 pGLuc:particle@PEI by 3T3 fibroblasts after 48 h of incubation (green: FITC-labeled
39
40 particles, blue : DAPI nuclei staining, scale bar = 20 µm) ; (C) Impact of PEI, particles
41
42 and particle@PEI systems on 3T3 cell viability after 4 h of contact as monitored by the
43
44 Alamar Blue test. Bar: 50µm.
45
46
47
48

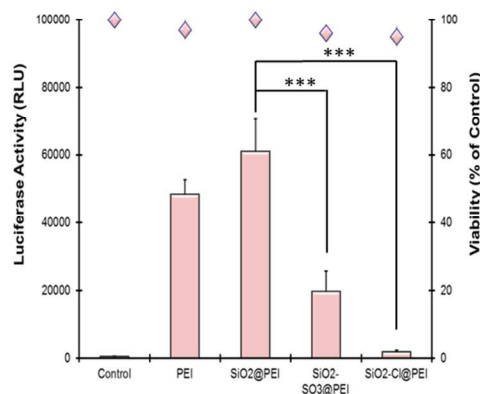
49
50 The transfection efficiency of the particles was evaluated in 3T3 mouse fibroblasts and
51
52 primary human keratinocytes using a plasmid encoding for Luciferase (pG-Luc) (**Figure**
53
54 **5**). Quantities of polymers used in this experiment were not toxic for cells with the aim of
55
56
57
58
59
60

1
2
3
4 comparing the abilities of transfection of the different systems. The ability of transfection
5
6 was first analyzed on immortalized 3T3 fibroblasts (**Figure 5a**). Among particles, the
7
8 highest bioluminescence level was obtained with SiO₂@PEI, that was one order of
9
10 magnitude below that of PEI alone.²⁵ The efficiency of SiO₂-SO₃@PEI particles was ten
11
12 times lower than that measured with SiO₂@PEI. Last, a very weak luciferase activity was
13
14 observed with the SiO₂-Cl@PEI system that was not statistically different from the
15
16 control.
17
18
19
20
21
22
23
24
25

(A)



(B)



55 **Figure 5:** Transfection of mouse 3T3 fibroblasts (A) and human primary keratinocytes
56
57 (B) after a 4 h incubation period with pGLuc :particle@PEI systems. Variance of the
58
59
60

1
2
3
4 luciferase expression among particle groups was determined by one-way ANOVA with
5
6
7 Tukey posthoc test (***) $P < 0.001$
8
9

10
11
12 Indeed, the luciferase activity was only the double of the basal level quantified in
13 controls samples (without pG-Luc). The potential of PEI@particles to delivery genes was
14 also investigated on primary normal human keratinocytes (**Figure 5b**). The
15 bioluminescence levels measured after incubation with the different systems of particles
16 revealed the same profiles of transfection as those observed in 3T3 cells. The best ability
17 of transfection was obtained with SiO₂@PEI. The transfection efficiency was three times
18 lower with SiO₂-SO₃@PEI particles and that measured with the SiO₂-Cl@PEI system
19 was very low. Compared with the performance of the different particles@PEI systems on
20 3T3 cells, the bioluminescence levels measured with keratinocytes were two times lower.
21
22
23
24
25
26
27
28
29
30
31
32
33
34
35

36 Despite their extensive study, the exact mechanisms driving cell transfection by
37 non-viral vectors are still controversial.³⁷ Yet the main steps of the process have been
38 identified. First, the DNA complex must be internalized by endocytosis, a process that
39 depends on its size and charge. Here, the three particles exhibit similar positive charges
40 compatible with internalization. SiO₂@PEI and Si-SO₃@PEI particles have similar
41 dimensions (*ca.* 200 nm) in PBS whereas SiO₂-Cl@PEI dispersions show a tendency to
42 aggregate into larger species (*ca.* 800 nm). Nevertheless fluorescence images suggest the
43 successful internalization of a fraction of SiO₂-Cl@PEI particles. This could be explained
44 by the de-aggregation of SiO₂-Cl@PEI, allowing the uptake of individual particles. A
45
46
47
48
49
50
51
52
53
54
55
56
57
58
59
60

1
2
3
4 second hypothesis relies on the polydispersity of SiO₂-Cl@PEI particles. According to
5
6 the results obtained by DLS, a small fraction of particles possesses the appropriate size
7
8 (less than 400 nm) to be engulfed by cells. Despite the fact that the uptake abilities are
9
10 cell dependent, it is generally admitted that particles larger than 500 nm are not likely to
11
12 be internalized by endocytosis in mammalian cells.^{19,38} This could explain the very low
13
14 level of transfection. The question of the particle size, rather the covalent bonding seems
15
16 to a crucial parameter for cellular uptake of SiO₂-Cl@PEI. Several groups have
17
18 functionalized PEI by covalent attachment on mesoporous silica nanoparticles or on
19
20 hyaluronic acid chains. They obtained particles:DNA complexes with a limited
21
22 aggregation (less than 350 nm), thereby permitting cellular uptake and transfection.³⁹⁻⁴¹
23
24 In addition, some of these particles were functionalized with mannose facilitating the
25
26 engulfment by receptor-mediated endocytosis.⁴⁰ Last, the studied cells were macrophages
27
28 that are cells with high efficiency of engulfment.
29
30
31
32
33
34
35
36
37
38

39 In a second step, DNA must be released in the cytoplasm.³⁷ This is possible via
40
41 endosome acidification leading to endosomal membrane disruption. The plasmid carrier
42
43 can play a role both in the destabilization of the endosome via the proton sponge effect
44
45 and in the protection of DNA against acidic degradation. The first effect increases with
46
47 the amount of PEI and should therefore be more favorable with SiO₂. The protecting
48
49 effect depends on the PEI quantity, its conformation and flexibility.¹⁰ The ratio PEI:DNA
50
51 for SiO₂@PEI , Si-SO₃@PEI, SiO₂-Cl@PEI were 3.8, 1.2 and 1.7, respectively.
52
53
54
55 According to the results of cell viability, these ratios were not associated with any
56
57
58
59
60

1
2
3
4 cytotoxicity. It is well-admitted that the transfection capabilities increase when the
5
6 PEI:DNA ratio rises.⁴² Hence, the quantity of PEI on SiO₂ particles could explain in part
7
8
9 its higher transfection ability because of its impact on DNA compaction and protection
10
11
12 against nucleases. Nevertheless, the conformation of PEI at the surface also plays an
13
14
15 important role and is expected to be optimal for the Si-SO₃@PEI system.
16

17
18 In a following step, the released plasmid must diffuse to the nucleus and enter, either
19
20 during mitosis or via the nuclear import machinery. Importantly, the stage at which PEI
21
22 and DNA are dissociated is still a matter of debate.³⁷ However, focusing on the
23
24
25 particle-PEI interactions, it is interesting to note that in the acidic conditions of the
26
27
28 endosomes, an important fraction of the silanolate groups of the bare silica particles
29
30
31 become protonated. This decreases the negative charge of the carrier, favoring PEI
32
33
34 desorption. On the opposite, sulfonate functions should remain negatively-charged,
35
36
37 preserving their attractive interactions with PEI. Finally, for SiO₂-Cl, the existing
38
39
40 covalent bonds are not expected to be cleaved, limiting the possibility for complexes to
41
42
43 escape. These trends in PEI detachment from particles nicely follow the measured
44
45
46 transfection efficiencies, suggesting that such a release is a relevant event in the plasmid
47
48
49 delivery process.

50
51 Surprisingly, the performance of PEI alone was not better than that of the
52
53 SiO₂@PEI system for keratinocytes, in contrast to the results obtained with 3T3 cells.
54
55
56 The highest cell transfection observed with PEI compared to particles on immortalized
57
58
59 cells could be explained by the particle size and the metabolic activity of 3T3 fibroblasts.
60

1
2
3
4 PEI/DNA complexes are about 100 nm in diameter.⁴³ These complexes are rapidly
5
6
7
8
9
10
11
12
13
14
15
16
17
18
19
20
21
22
23
24
25
26
27
28
29
30
31
32
33
34
35
36
37
38
39
40
41
42
43
44
45
46
47
48
49
50
51
52
53
54
55
56
57
58
59
60

PEI/DNA complexes are about 100 nm in diameter.⁴³ These complexes are rapidly
uptaken by cells *via* the clathrin-mediated endocytosis. In contrast, larger particles@PEI
systems are more internalized by the caveolin-mediated endocytosis.⁴⁴ Therefore the
clathrin pathway seems to be more efficient in 3T3 fibroblasts to engulf complexes.
Second, 3T3 cells proliferate rapidly, facilitating plasmid transfer by disruption of the
nuclear membrane during cell division. Thus it can be proposed that PEI complexes are
rapidly uptaken, transported to the nucleus and that protein expression occurs at a very
high rate thanks to fast proliferation. In contrast, the uptake of particles being less
efficient, there is a delay required for sufficient plasmid accumulation before significant
protein expression is achieved. In the case of primary cells such as keratinocytes, the cells
proliferate at a lower rate. Therefore the overall protein expression rate is slower for both
systems. Moreover, in these conditions, it is possible for silica particles to accumulate in
a higher quantity between two cellular division event, so that the protein expression level
becomes comparable to that of PEI.

CONCLUSION

These results provide an important insight on the relationship between the chemistry of
silica nanoparticles and their biological properties as gene delivery vectors. Whereas great
attention has already been paid to the optimization of the plasmid loading, we have here
enlightened the influence of the chemistry of the particle surface on the conformation and
lability of the cationic coating. Such effects were observed for both immortalized and

1
2
3
4 primary mammalian cells. Our findings particularly suggest that a delicate balance has to
5
6
7 be established between weak particle/coating and strong coating/plasmid interactions.
8
9
10 They therefore provide interesting guidelines for further optimization of
11
12 nanoparticle-based gene carriers but also, on a more general level, for the design of
13
14 nanovectors for intracellular delivery of bioactive molecules.
15
16
17
18
19

20 ASSOCIATED CONTENT

21
22 **Supporting Information.** TEM images (**Figure S1**), ^{13}C IRCP-MAS spectra (**Figure**
23
24 **S2**), full XPS spectra (**Figure S3**). This material is available free of charge via the
25
26 Internet at <http://pubs.acs.org>.
27
28
29
30
31
32
33

34 AUTHOR INFORMATION

35
36
37 **Corresponding Authors.** *Email: thibaud.coradin@upmc.fr;
38
39 christophe.helary@upmc.fr
40
41
42
43
44

45 ACKNOWLEDGMENTS

46
47 X.W. PhD grant was funded by the China Scholarship Council. The authors thank C.
48
49 Aimé (LCMCP) for fruitful discussions and C. Méthivier (UPMC) for the XPS
50
51 experiments.
52
53
54
55
56
57
58
59
60

REFERENCES

- 1
2
3
4
5
6
7 (1) Cartier, N.; Hacein-Bey-Abina, S.; Bartholomae, C.C.; Veres, G.; Schmidt, M.;
8
9 Kutschera, I.; Vidaud, M.; Abel, U.; Dal-Cortivo, L.; Caccavelli, L.; Mahlaoui, N.;
10
11 Kiermer, V.; ittelstaedt, D.; Bellesme, C.; Lahlou, N.; Lefrere, F.; Blanche, S.; Audit,
12
13 M.; Payen, E.; Leboulch, P.; l'Homme, B.; Bougneres, P.; Von Kalle, C.; Fischer, A.;
14
15 Cavazzana-Calvo, M.; Aubourg, P. Hematopoietic stem cell gene therapy with a lentiviral
16
17 vector in X-linked adrenoleukodystrophy. *Science*, **2009**, *326*, 818-823.
18
19
20
21
22 (2) Kay, M. A.; Manno, C. S.; Ragni, M. V.; Larson, P. J.; Couto, L. B.; McClelland, A.;
23
24 Glader, B.; Chew, A. J.; Tai, S. J.; Herzog, R. W.; Arruda, V.; Johnson, F.; Scallan, C.;
25
26 Skarsgard, E.; Flake, A.W.; High, K. A. Evidence for gene transfer and expression of
27
28 factor IX in haemophilia B patients treated with an AAV vector. *Nature Genetics*, **2000**,
29
30
31
32
33
34
35
36
37 (3) De Laporte, L.; Huang, A.; Ducommun, M. M.; Zelivyanska, M. L.; Aviles, M. O.;
38
39 Adler, A. F.; Shea, L. D. Patterned transgene expression in multiple-channel bridges after
40
41 spinal cord injury. *Acta Biomater.*, **2010**, *6*, 2889-2897.
42
43
44 (4) Kofron, M.D.; Laurencin, C. T. Bone tissue engineering by gene delivery. *Adv. Drug*
45
46
47
48
49
50 (5) Zhang, Y.; Wang, Z.; Gemeinhart, R. A. Progress in microRNA delivery. *J Control.*
51
52
53
54
55
56
57
58
59
60

- 1
2
3
4 (6) Bonadio, J.; Smiley, E.; Patil, P.; Goldstein, S. Localized, direct plasmid gene
5
6 delivery in vivo: prolonged therapy results in reproducible tissue régénération. *Nat. Med.*
7
8
9 **1999**, *5*, 753-759.
10
11
12 (7) Davidson, B. L.; McCray, P. B., Jr. Current prospects for RNA interference-based
13
14 therapies. *Nat. Rev. Genetics* **2011**, *12*, 329-340
15
16
17 (8) Seidlits, S. K.; Gower, R. M.; Shepard, J. A.; Shea, L. D. Hydrogels for lentiviral
18
19 gene delivery. *Expert Opin Drug Deliv.* **2013**, *10*, 499–509.
20
21
22 (9) Aied, A.; Greiser, U.; Pandit, A.; Wang, W. Polymer gene delivery: overcoming the
23
24 obstacles. *Drug Discov. Today*, **2013**, *18*, 1090-1098.
25
26
27
28 (10) Godbey, W. T.; Wu, K. K.; Mikos, A. G. Poly(ethylenimine) and Its Role in Gene
29
30 Delivery. *J. Controlled Release* **1999**, *60*, 149-160.
31
32
33 (11) Patnaik, S.; Gupta, K. C. Novel polyethylenimine-derived nanoparticles for in vivo
34
35 gene delivery. *Expert Opin. Drug Del.* **2013**, *10*, 215-228.
36
37
38 (12) Guo, X.; Huang, L. Recent Advances in Nonviral Vectors for Gene Delivery. *Acc.*
39
40 *Chem. Res.* **2012**, *45*, 971-979.
41
42
43 (13) Hartono, S. B.; Gu, W.; Kleitz, F.; Liu, J.; He, L.; Middelberg, A. P. J.; Yu, C.; Lu,
44
45 G. Q.; Qiao, S. Z. Poly-l-lysine Functionalized Large Pore Cubic Mesostructured Silica
46
47 Nanoparticles as Biocompatible Carriers for Gene Delivery. *ACS Nano* **2012**, *6*,
48
49 2104-2117.
50
51
52
53
54
55
56
57
58
59
60

- 1
2
3
4 (14) Fuller, J. E.; Zugates, G. T.; Ferreira, L. S.; Ow, H. S.; Nguyen, N. N.; Wiesner, U.
5
6
7 B.; Langer, R. S. Intracellular delivery of core-shell fluorescent silica nanoparticles.
8
9
10 *Biomaterials* **2008**, *29*, 1526-1532.
- 11
12 (15) Luo, D.; Saltzman, W. M. Enhancement of transfection by physical concentration of
13
14
15 DNA at the cell surface. *Nat. Biotech.* **2000**, *18*, 893-895.
- 16
17
18 (16) He, L.; Feng, L.; Cheng, L.; Liu, Y.; Li, Z.; Peng, R.; Li, Y.; Guo, L.; Liu, Z.
19
20
21 Multilayer dual-polymer-coated upconversion nanoparticles for multimodal imaging and
22
23
24 serum-enhanced gene delivery. *ACS Appl. Mater. Interfaces* **2013**, *5*, 10381-10388.
- 25
26 (17) Mamaeva, V.; Sahlgren, C.; Lindén, M. Mesoporous silica nanoparticles in
27
28
29 medicine—Recent advances. *Adv. Drug Del. Rev.* **2013**, *65*, 689-702.
- 30
31 (18) Tang, F.; Li, L.; Chen, D. Mesoporous Silica Nanoparticles: Synthesis,
32
33
34 Biocompatibility and Drug Delivery. *Adv. Mater.* **2012**, *24*, 1504–1534.
- 35
36 (19) Mao, Z.; Zhou, X.; Gao, C. Influence of structure and properties of colloidal
37
38
39 biomaterials on cellular uptake and cell functions. *Biomater. Sci.* **2013**, *1*, 896-911.
- 40
41 (20) Lay, C.-Y.; Trewyn, B. G.; Jeftinija, D. M.; Xu, S.; Jeftinija, S.; Lin, V. S.
42
43
44 Mesoporous Silica Nanosphere-Based Carrier System with Chemically Removable CdS
45
46
47 Nanoparticle Caps for Stimuli-Responsive Controlled Release of Neurotransmitters and
48
49
50 Drug Molecules. *J. Am. Chem. Soc.* **2003**, *125*, 4451–4459.
- 51
52 (21) Kecht, J.; Schlossbauer, A.; Bein, T. Selective Functionalization of the Outer and
53
54
55 Inner Surfaces in Mesoporous Silica Nanoparticles. *Chem. Mater.* **2008**, *20*, 7207-7214.
56
57
58
59
60

- 1
2
3
4 (22) Xia, T.; Kovoichich, M.; Liong, M.; Meng, H.; Kabehie, S.; George, S.; Zink, J. I.;
5
6
7 Nel, A. E. Polyethyleneimine Coating Enhances the Cellular Uptake of Mesoporous
8
9
10 Silica Nanoparticles and Allows Safe Delivery of siRNA and DNA Constructs. *ACS*
11
12 *Nano* **2009**, *3*, 3273-3286.
13
14 (23) Yu, M.; Niu, Y.; Yang, Y.; Hartono, S. B.; Yang, J.; Huang, X.; Thorn, P.; Yu, C. An
15
16
17 Approach to Prepare Polyethylenimine Functionalized Silica-Based Spheres with Small
18
19
20 Size for siRNA Delivery. *ACS Appl. Mater & Inter.* **2014**, *6*, 15626-15631.
21
22
23 (24) Stöber, W.; Fink, A.; Bohn, E. Controlled growth of monodisperse silica spheres in
24
25
26 the micron size range. *J. Colloid Interface Sci.* **1968**, *26*, 62-69.
27
28 (25) Wang, X.; Helary, C.; Coradin, T. Local and Sustained Gene Delivery in
29
30
31 Silica-Collagen Nanocomposites. *ACS Appl. Mater & Inter.* **2015**, *7*, 2503-2511
32
33
34 (26) Aimé, C.; Mosser, G.; Pembouong, G.; Bouteiller, L.; Coradin, T. Controlling the
35
36
37 nano–bio interface to build collagen–silica self-assembled networks. *Nanoscale* **2012**, *4*,
38
39 7127-7134.
40
41 (27) Ellman G.L. Tissue sulfhydryl groups. *Arch. Biochem. Biophys.* **1959**, *82*, 70–73
42
43
44 (28) Quignard, S.; Mosser, G.; Boissière, M.; Coradin, T. Long-term fate of silica
45
46
47 nanoparticles interacting with human dermal fibroblasts. *Biomaterials* **2012**, *33*,
48
49 4431-4442
50
51
52 (29) Louette, P.; Bodino, F.; Pireaux, J.-J. Poly-ethylene imine (PEI) XPS Reference
53
54
55 Core Level and Energy Loss Spectra. *Surface Sci. Spectra*, **2005**, *12*, 54-58
56
57
58 (30) Shchukarev, A.; Rosenqvist, J.; Sjöberg, S. XPS study of the silica–water interface.
59
60

1
2
3
4 *J. Electron Spectr. Related Phenom.* **2004**, 137-140, 171-176

5
6
7 (31) Islam, Md. S.; Choi, W. S.; Lee, H.-J. Controlled Etching of Internal and External
8 Structures of SiO₂ Nanoparticles Using Hydrogen Bond of Polyelectrolyte. *ACS Appl.*
9 *Mater. Interfaces* **2014**, 6, 9563–9571

10
11
12 (32) Nasef, N. N.; Saidi, H.; Nor, H. M.; Yarmo, M. A. XPS Studies of Radiation Grafted
13 PTFE-g-polystyrene Sulfonic Acid Membranes. *J. Appl. Polym. Sci.* **2000**, 76, 336–349

14
15
16 (33) Tsiourvas, D.; Tsetsekou, A.; Arkas, M.; Diplas, S.; Mastrogianni, E. Covalent
17 attachment of a bioactive hyperbranched polymeric layer to titanium surface for the
18 biomimetic growth of calcium phosphates. *J. Mater. Sci. Mater. Med.* **2011**, 22, 85-96.

19
20
21 (34) Nagaya, J.; Homma, M.; Tanioka, A.; Minakata, A. Relationship between
22 protonation and ion condensation for branched poly(ethylenimine). *Biophys. Chem.* **1996**,
23 60, 45-51.

24
25
26 (35) Leung, K.; Nielsen, I. M. B.; Criscenti, L. J. Elucidating the Bimodal Acid–Base
27 Behavior of the Water–Silica Interface from First Principles. *J. Am. Chem. Soc.* **2009**,
28 131, 18358-18365.

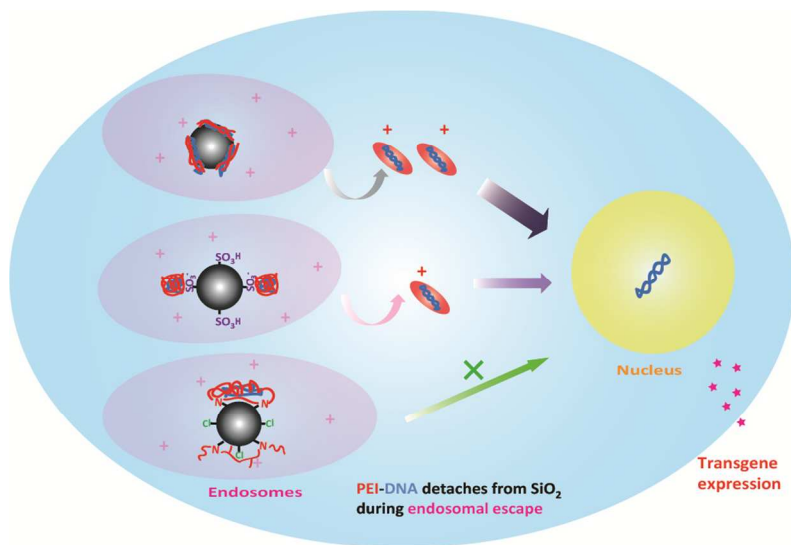
29
30
31 (36) Wightman, L.; Kircheis, R.; Rossler, V.; Carotta, S.; Ruzicka, R.; Kursa, M.;
32 Wagner, E. Different Behavior of Branched and Linear Polyethylenimine for Gene
33 Delivery In vitro and In vivo. *J. Gene Med.* **2001**, 3, 362-372.

34
35
36 (37) Won, Y.-Y.; Sharma, R.; Konieczny, S. F. Missing pieces in understanding the
37 intracellular trafficking of polycation/DNA complexes. *J. Controlled Release* **2009**, 139,
38 88-93.

- 1
2
3
4 (38) Wang, Z. J.; Tiruppathi, C.; Minshall, R. D; Malik, A., B. Size and dynamics of
5
6 caveolae studied using nanoparticles in living endothelial cells. *ACS Nano*. **2009**, *3*,
7
8 4110-4116.
9
10
11 (39) Buchman, Y. K.; Lellouche, E.; Zigdon, S.; Bechor, M.; Michaeli, S.; Lellouche,
12
13 J.-P. Silica Nanoparticles and Polyethyleneimine (PEI)-Mediated Functionalization: A
14
15 New Method of PEI Covalent Attachment for siRNA Delivery Applications.
16
17 *Bioconjugate Chem.* **2013**, *24*, 2076-2087.
18
19
20 (40) Park, I. Y. ; Kim, I. Y. ; Yoo, M. K. ; Choi, Y. J. ; Cho, M. H. ; Cho, C. S.
21
22 Mannosylated polyethylenimine coupled mesoporous silica nanoparticles for
23
24 receptor-mediated gene delivery. *Int. J. Pharm.* **2008**, *359*, 280-287.
25
26
27 (41) Jiang, G.; Park, K.; Kim, J.; Oh, E. J.; Kang, H.; Han, S.-E.; Oh Y.-K; Park, T. G;
28
29 Hahn, S., K. Hyaluronic acid-polyethyleneimine conjugate for target specific intracellular
30
31 delivery of siRNA. *Biopolymers* **2008**, *89*, 635-642.
32
33
34 (42) Huang, Y. C. ; Connell, M. ; Park, Y. ; Mooney, D. J. ; Rice, K. G. Fabrication and
35
36 in vitro testing of polymeric delivery system for condensed DNA. *J. Biomed Mater. Res.*
37
38 *A.* **2003**, *67*, 1384-1392.
39
40
41 (43) Fischer, D.; Bieber, T.; Li, Y. X.; , Elsasser, H. P.; Kissel, T. A novel non-viral
42
43 vector for DNA delivery based on low molecular weight, branched polyethyleneimine:
44
45 Effect of molecular weight on transfection efficiency and cytotoxicity. *Pharmaceut Res.*
46
47
48
49
50
51
52
53
54
55
56
57
58
59
60

1
2
3
4 (44) Rejman, J.; Oberle, V.; Zuhorn, I. S.; Hoekstra, D. Size-dependent Internalization of
5
6
7 Particles via the Pathways of Clathrin- and Caveolae-mediated Endocytosis. *Biochem. J.*
8
9
10 **2004**, 377, 159-169.
11
12
13
14
15
16
17
18
19
20
21
22
23
24
25
26
27
28
29
30
31
32
33
34
35
36
37
38
39
40
41
42
43
44
45
46
47
48
49
50
51
52
53
54
55
56
57
58
59
60

TOC graphics



Impact of Polyethyleneimine Conjugation Mode on the Cell Transfection Efficiency of Silica Nanovectors

Xiaolin Wang, Sylvie Masse, Guillaume Laurent, Christophe H elary,* and Thibaud

Coradin*

Sorbonne Universit es, UPMC Univ Paris 06, CNRS, UMR 7574, Laboratoire de Chimie de la Mati re Condens e de Paris, F-75005 Paris, France

*Corresponding Author: Email: thibaud.coradin@upmc.fr

Supporting Information

S1. Detailed experimental protocols

Figure S1. TEM images of nanoparticles

Figure S2. XPS spectra of nanoparticles

Figure S3. Agarose gel electrophoresis

Figure S4. ¹³C IRCP-MAS NMR spectra

Figure S5. Cell viability at the end of transfection experiments

S1. Detailed experimental protocols

Silica-polyethyleneimine particle preparation. Silica nanoparticles SiO₂ were synthesized by Stöber method using ammonia for the hydrolysis and polymerization of tetraethylorthosilicate (TEOS, Sigma). The amount of chemicals was shown in the table below.

TEOS (mL)	Ethanol (mL)	H ₂ O (mL)	Ammonia (25%, mL)
7.6	200	5.9	9.7

For SiO₂@PEI particle preparation, 200 mg of branched polyethyleneimine PEI (25 kDa) was dissolved in 20 mL of saline phosphate buffer (PBS, 10 mM, pH 7.4). Silica nanoparticle suspension in PBS (20 ml) was then added dropwise into the PEI solution under stirring. The mixtures were stirred for 48 h and particles were recovered by centrifugation, washed 3 times in PBS and finally resuspended in PBS.

For SiO₂-SO₃@PEI particle preparation, the SiNP was first functionalized with thiol groups by silylation with 3-mercaptopropyltrimethoxysilane (MPTMS). Typically, 1 g of silica was dispersed in a mixture of 100 ml ethanol and 2.2 ml ammonium hydroxide solution before addition of 1 ml MPTMS. The mixture was stirred for 40 min at room temperature. Subsequently, the reaction mixture was heated to 80 °C and the total volume was reduced by 2/3 by distillation of ethanol and ammonia at ambient pressure. Then, the mixture was cooled back to room temperature, centrifuged, washed 3 times with ethanol and dried at 60 °C. Then 0.9 g of the thus-obtained SiO₂-SH was suspended in 45 mL

hydrogen peroxide (H_2O_2 35%, Acros Organics) under stirring at RT for 48 hours. The solid product was washed by centrifugation with distilled water before addition of 35 mL of concentrated sulfuric acid (H_2SO_4 95.0-98.0%, Sigma Aldrich) and stirred for 2 hours at RT. Finally the as-synthesized $\text{SiO}_2\text{-SO}_3$ particles were washed with water, suspended in PBS and coated with PEI as described above.

For $\text{SiO}_2\text{-Cl@PEI}$ particle preparation, 400 mg of SiO_2 nanoparticles was dispersed in 20 mL of dried toluene, and 1.3 mL of chloropropyltriethoxysilane (Cl-PTES) was added to the suspension, that was further kept under reflux for 24 h. The product was washed thoroughly with toluene and ethanol, and dried at room temperature. Then, 200 mg $\text{SiO}_2\text{-Cl}$ was dispersed in 20 ml ethanol, and 0.8 g of PEI was added to the suspension. The suspension was refluxed for 24 h. The final solid product was recovered by washing with ethanol and dried at room temperature. The as-synthesized SiNP-Cl@PEI was suspended in 10 mM PBS (pH 7.4) before use.

Characterizations of $\text{SiO}_2\text{-X@PEI}$ Particle. Sizes and zeta potential (ζ) were measured in 10 mM PBS solution using a ZetaSizer Nano (Malvern Instruments Ltd., Worcestershire, UK). Particles were also imaged using Transmission Electron Microscopy (TEM) on a JEOL 1011 instrument. The amount of adsorbed PEI was determined by elemental analysis (C,H,O,N). Specially, for $\text{SiO}_2\text{-SO}_3$, the amount of SO_3 was calculated according to the amount of $-\text{SH}$ before oxidation, which is determined by Ellman test. For this test, a phosphate buffer (0.2 M, pH = 7.3) was prepared and labeled as solution A. Solution B (10 mM EDTA) was produced by dissolving 372 mg of EDTA

in 100 mL of solution A, and solution C(6 mM DTNB) was prepared by dissolving 238 mg of DTNB in 100 mL of solution A. Several vials were filled with a mixture of 8 ml of solution A, 1 mL of solution B and 1 mL of solution C. A series of masses of SiO₂-SH, less than 50 mg, were measured and then each dispersed into a vial mixture solution. Simultaneously, several known quantities of thiol (obtained from a solution of MPTMS) were also introduced in the same mixture solution to determine the molar extinction coefficient by linear regression. After 45 minutes of stirring, the particle dispersion is filtered through a syringe filter. The absorbance of the filtrate and standard MPTMS solutions are determined by spectroscopy. The absorbance of the solutions MTPMS can be traced back to the value for the experience of the molar extinction coefficient of NTB²⁻ by linear regression. It can then inform the thiol concentration, therefore sulfonates, on the surface of our particles.

pDNA-PEI and pDNA-SiO₂-X@PEI Complexation. Reporter plasmid pCMV-GLuc (pGluc) encoding Gaussia Luciferase (New England BioLabs, Ipswich, MA) was used to quantify transgene expression. This plasmid was amplified by one shot[®] BL21(DE3) pLysS kit (Invitrogen[™], Life technologies), extracted by one PureLink[®] HiPure Plasmid kit (Invitrogen[™], Life technologies) and finally stored in Tris-EDTA buffer at -20 °C. pDNA-PEI complexes were prepared at weight ratio of 1:2. pDNA-SiO₂-X@PEI (X = none, SO₃, Cl) complexes were prepared at various pDNA: SiO₂-X@PEI weight ratios. Complexes formation was examined by agarose gel

electrophoresis. Briefly, 1 μL of pDNA solution ($0.1 \mu\text{g} \cdot \mu\text{L}^{-1}$) were mixed homogeneously with a total volume of 9 μL of SiO₂-X@PEI suspension or PEI solution (PBS 1x) by vortexing in a microcentrifuge tube. The resulting mixtures were left at room temperature for 2 h to achieve complete complexation, before being loaded onto 0.7% agarose gel with ethidium bromide ($0.1 \mu\text{g} \cdot \text{mL}^{-1}$) and running with TAE buffer at 100 V for 40 min. DNA retardation was observed by irradiation with ultraviolet light.

Cell Transfection and Cell Viability. 3T3 mouse fibroblasts were cultured in complete cell culture medium (Dulbecco's Modified Eagle's Medium (DMEM) supplemented with 10% fetal serum, $100 \text{ U} \cdot \text{mL}^{-1}$ penicillin, $100 \mu\text{g} \cdot \text{mL}^{-1}$ streptomycin and $0.25 \mu\text{g} \cdot \text{mL}^{-1}$ Fungizone). Tissue culture flasks (75 cm^2) were kept at 37°C in a 95 % air: 5 % CO₂ atmosphere. Before confluence, fibroblasts were removed from culture flasks by treatment with 0.1% trypsin and 0.02 % EDTA. Cells were rinsed and resuspended in the above culture medium before use.

Transfection efficiency of pDNA-PEI and pDNA-SiO₂-X@PEI were evaluated by luciferase expression of pGLuc by 3T3 mouse fibroblast cells in cell culture medium. The cells were plated at a density of $5 \cdot 10^4$ per well in a 24-well plate. pDNA-PEI or pDNA-PEI-SiO₂-X complexes (25 μL) were added to the cell culture medium. After 4 h, the supernatant was removed, the well was refreshed with 1 mL complete medium and the cells were then cultured for another 44 h for the expression of luciferase. For measurements of luciferase activity, a BioLux Gaussia Luciferase Assay Kit (New England Biolabs) was used and transgene expression of luciferase was reported as

relative light units (RLU). Control groups were under the same culture condition as the experiment groups except for the absence of DNA complexes.

Internalization of nanoparticles in 3T3 mouse fibroblasts was studied using fluorescence microscopy. Fluorescent particles were obtained following the previously described protocol except for the addition of a solution of fluorescein-grafted aminopropyl triethoxysilane (APTES, Merck ; FITC isomer 1 95%, Alpha Aesar). The pDNA-particle complexes were incubated with cells for 24 h. The cell culture medium was removed and the cells were rinsed 3 times with PBS and fixed with 4% paraformaldehyde for 1 hour at RT. The cell nucleus was then stained with DAPI (4',6-diamidino-2-phenylindole dihydrochloride, Life technologies, 300 nM in PBS) for 10 min and rinsed with PBS before observation.

Cell viability was monitored using the Alamar Blue test as a function of particle dose after 4 h of contact and after transfection. In all cases, 200 μ L of the Alamar Blue solution (10% in cell culture medium) was added to 1 mL of the cell culture medium. The cells were then incubated at 37 °C with 5 % CO₂ for 4 h. The supernatant in each well was then collected, diluted with 800 μ L water, and its absorbance was measured at $\lambda = 570$ nm and 600 nm. Cell viability was calculated and reported as a percentage of the control group (n = 6).

Figure S1. TEM images of SiO₂, SiO₂-SO₃, SiO₂-Cl before(A-C) and after (D-F) modification with PEI 25 kDa

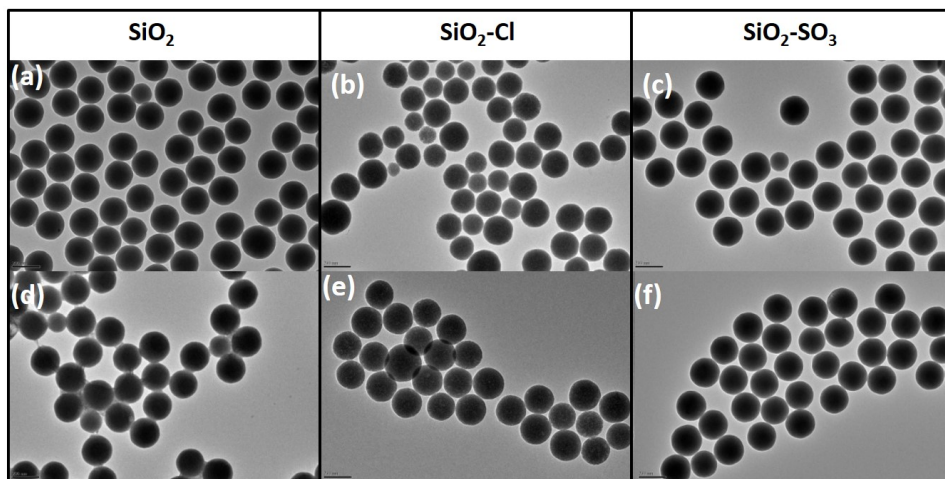
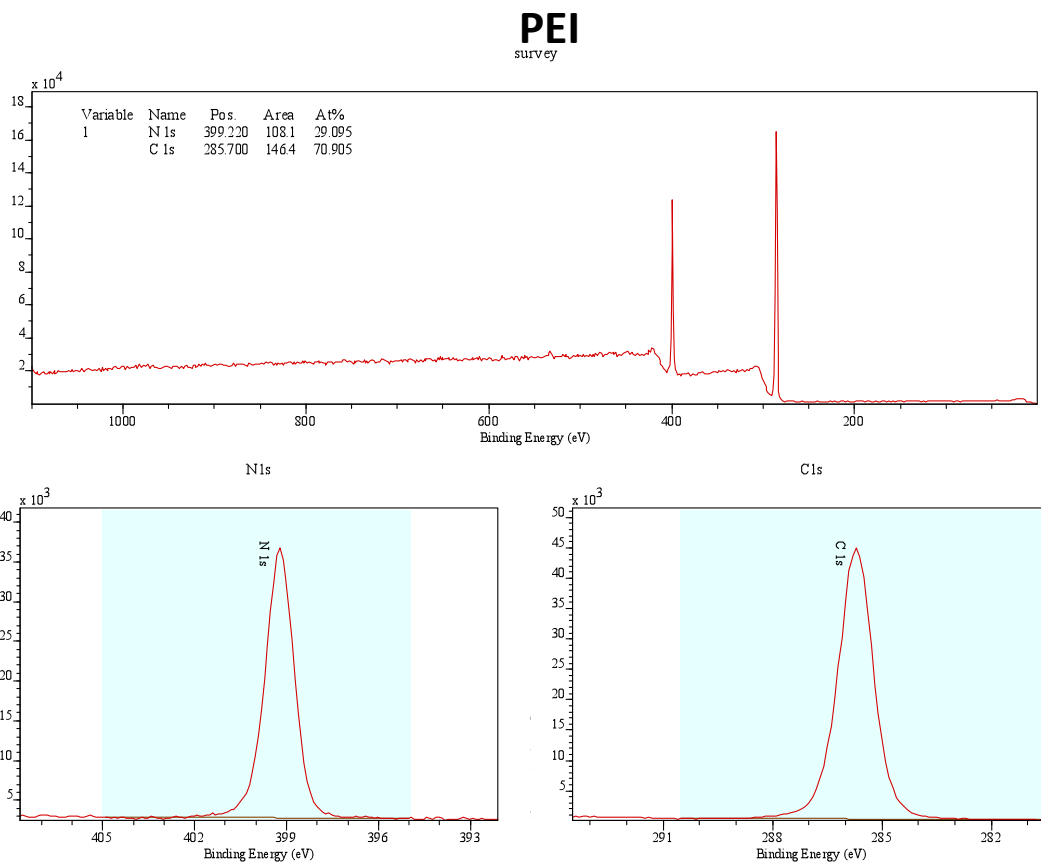
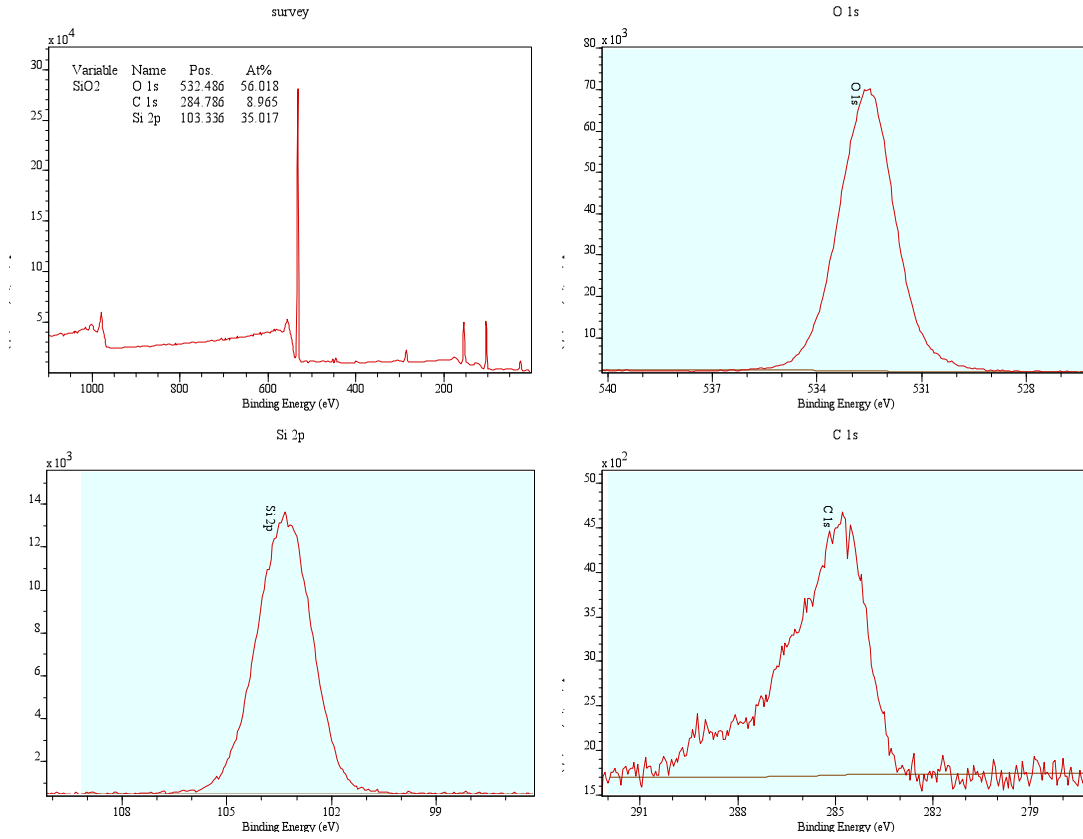


Figure S2. XPS spectra for SiO₂, SiO₂-SO₃, SiO₂-Cl before and after modification with PEI 25 kDa. PEI 25 kDa was used for comparison

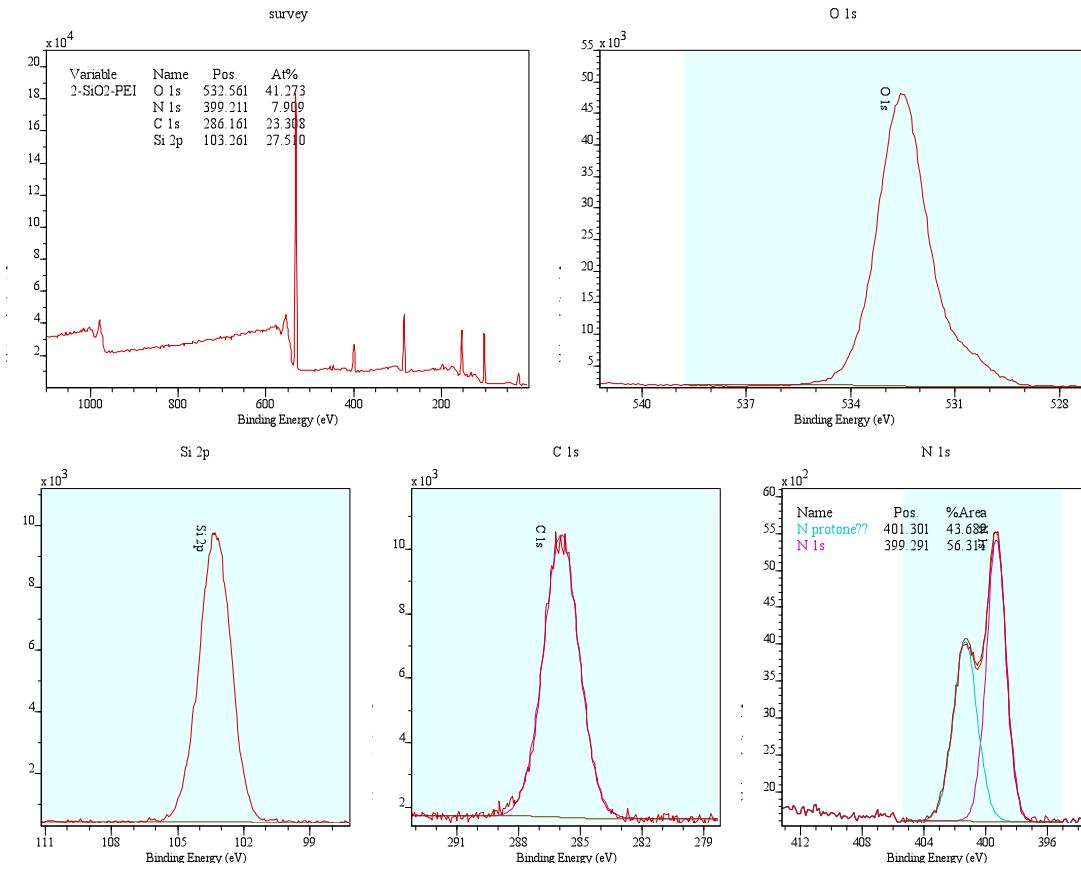


SiO₂

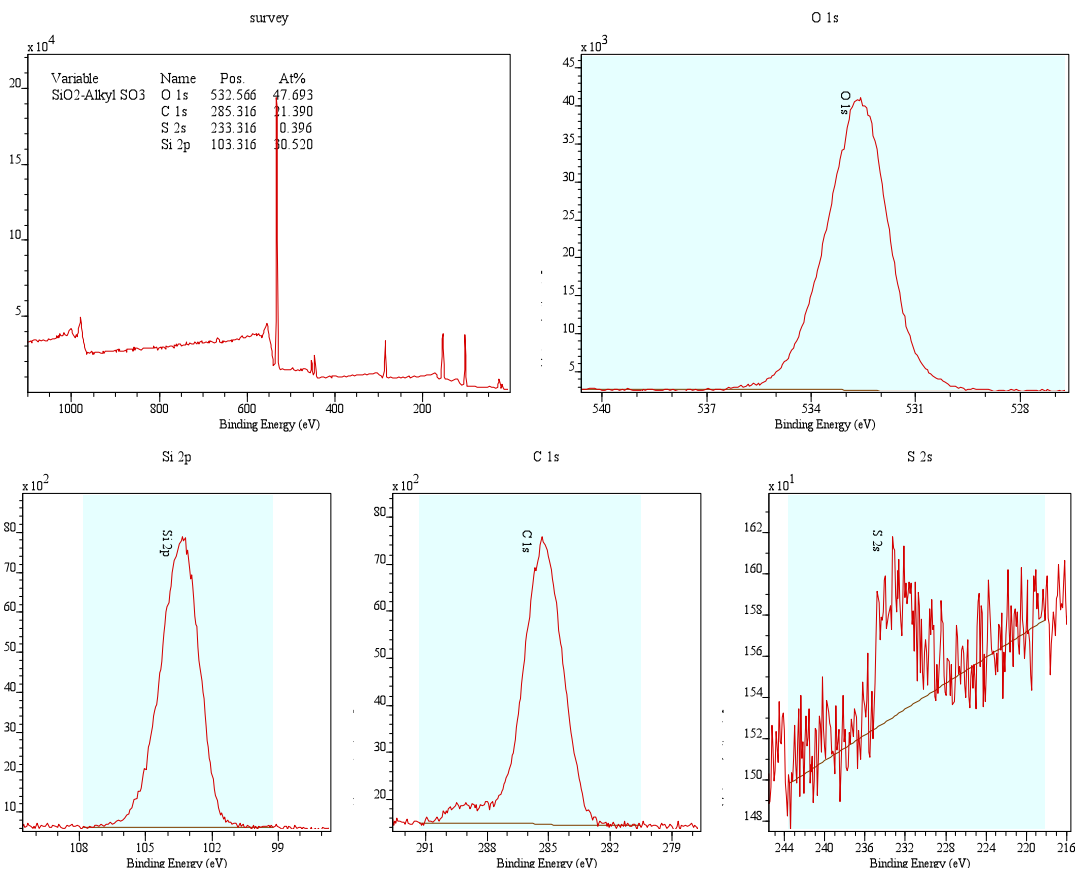


CasaXPS (This string can be edited in CasaXPS DEF/PrintFootNote.txt)

SiO₂@PEI

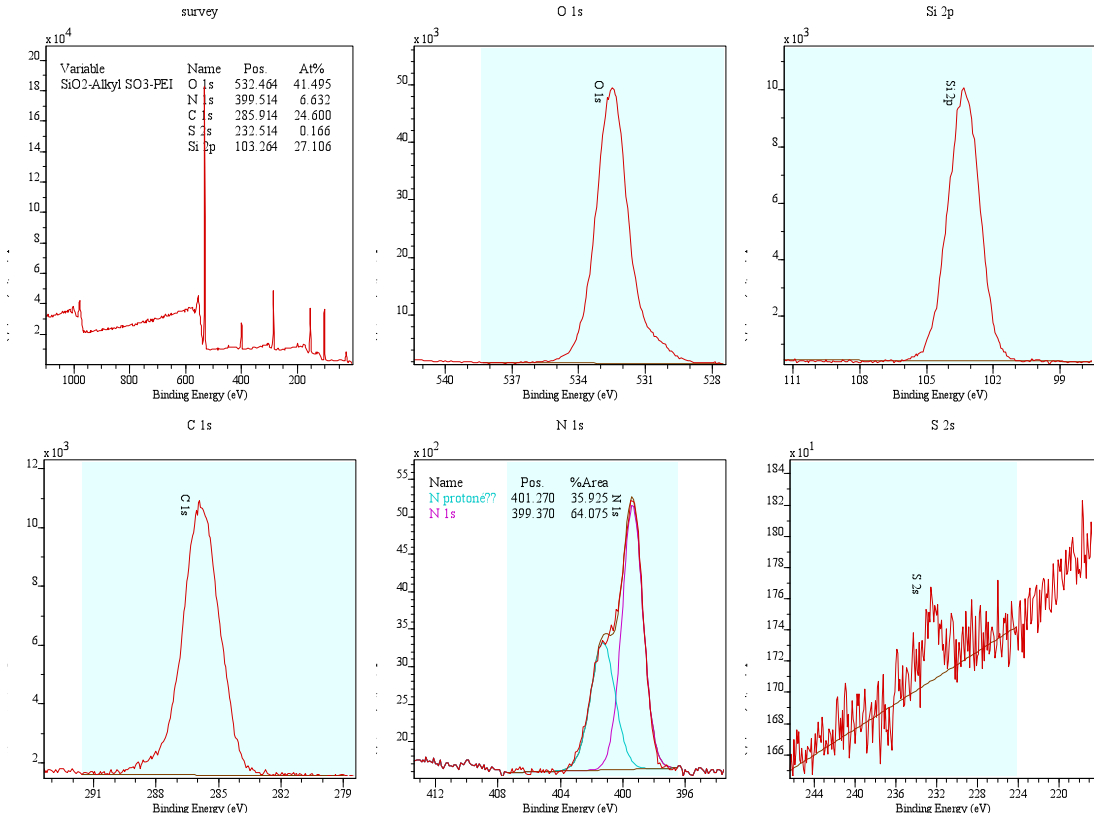


SiO₂ -SO₃



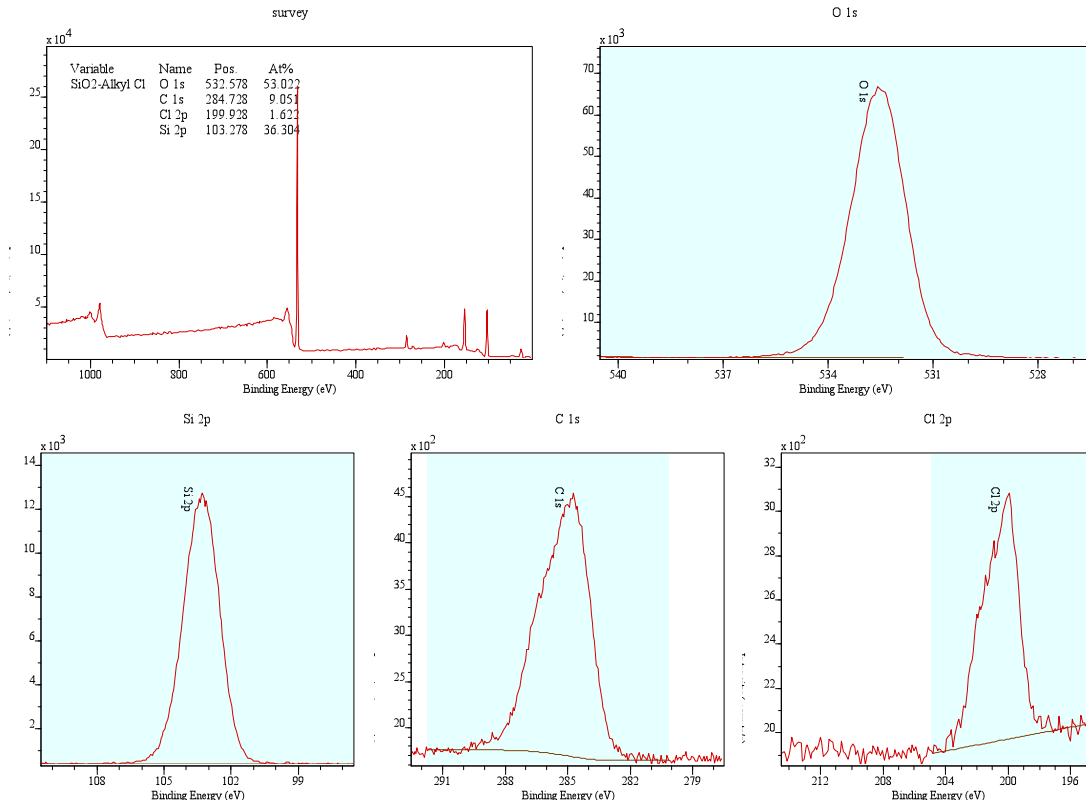
CasaXPS (This string can be edited in CasaXPS.DEF/PrintFootNote.txt)

SiO₂ -SO₃@PEI

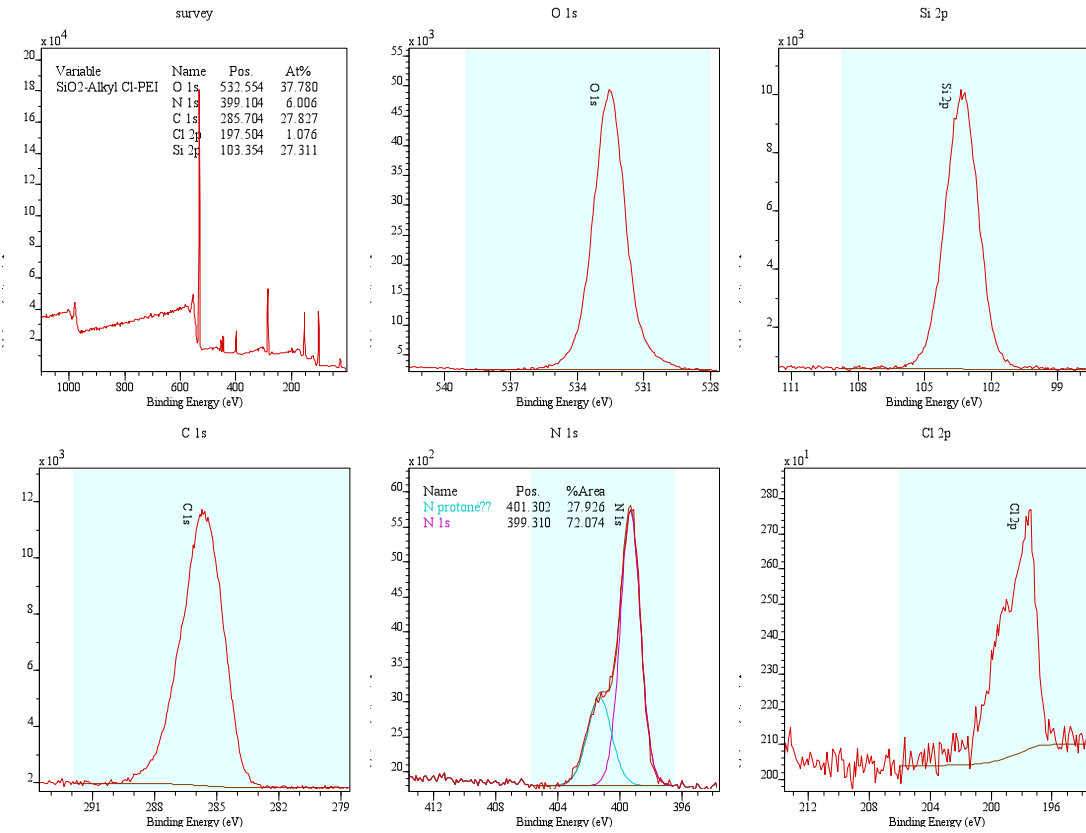


CasaXPS (This string can be edited in CasaXPS DEF/PrintFootNote.txt)

SiO₂ -Cl



SiO₂ -Cl@PEI



CasaXPS (This string can be edited in CasaXPS/DEF/PrintFootNote.txt)

Figure S3. Agarose gel electrophoresis showing the influence of PEI conjugation mode on pGLuc complexation. A constant amount of pGLuc was complexed with particles at 1:3, 1:10, 1:30 and 1:50 weight ratios.

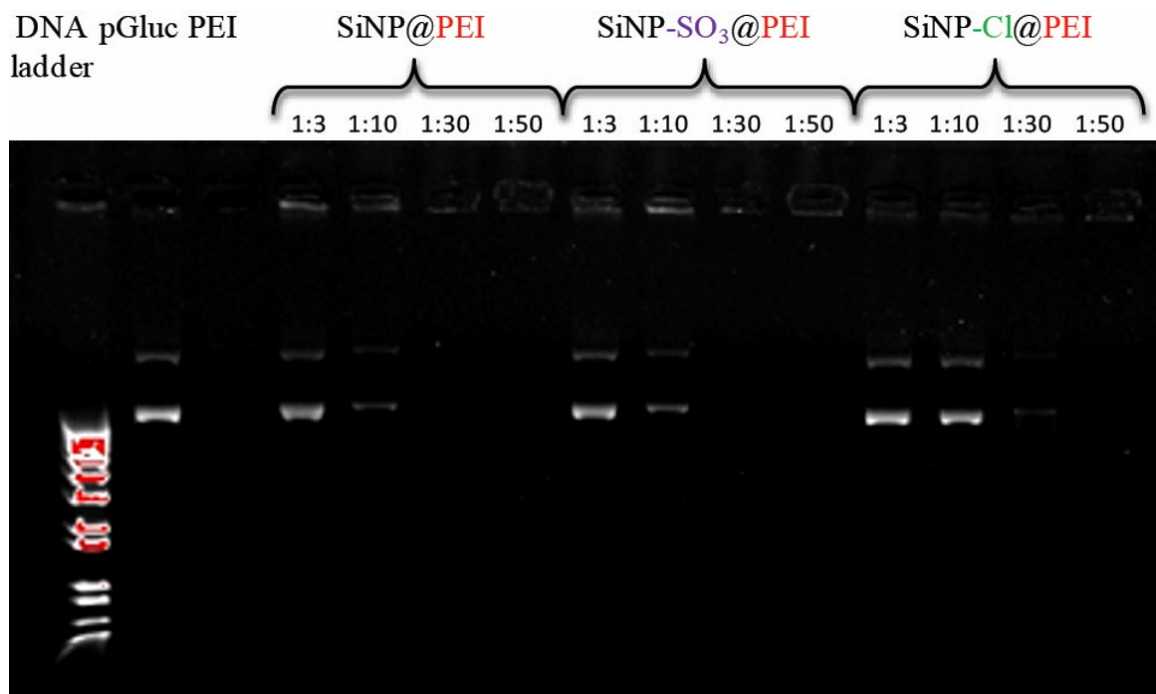
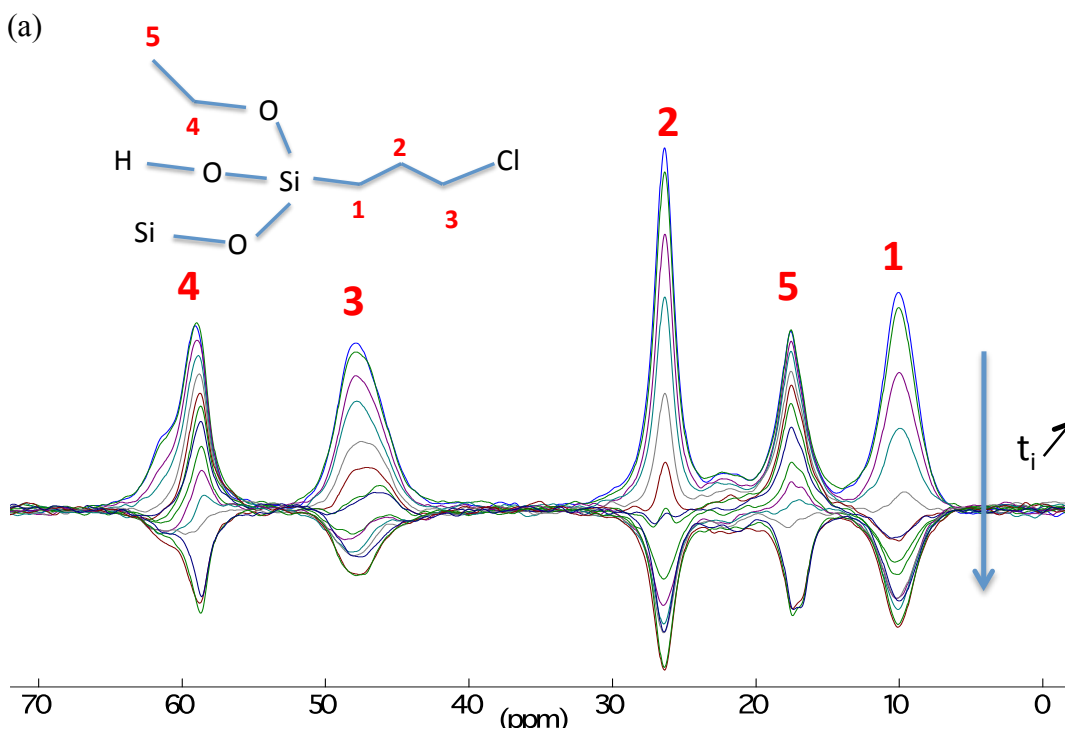


Figure S4. ^{13}C Inversion recovery cross polarization (IRCP)-MAS NMR spectra of (a) $\text{SiO}_2\text{-Cl}$ and (b) $\text{SiO}_2\text{-Cl@PEI}$. Main acquisition parameters used for the IRCP exp.:
 Recycle time: 1s; contact time: 1ms; NS: 4096; ro: 5 kHz; inversion time t_i (from top to bottom): 5, 10, 20, 30, 50, 70, 100, 200, 300, 500, 700, 1.000, 3.000, 5.000, 10.000 μs .
 In $\text{SiO}_2\text{-Cl}$, the signal of the C(3) in α position of the Cl atom reverses for an inversion time of 200-300 μs ; in $\text{SiO}_2\text{-Cl@PEI}$, the C(3) signal reverses for an inversion time of 50-70 μs . The faster cross-polarization rate indicates a decrease in mobility of the C(3) upon interaction with PEI (D.G Cory, W.M. Ritchey, *Macromolecules*, **1989**, 22, 1611-16615)



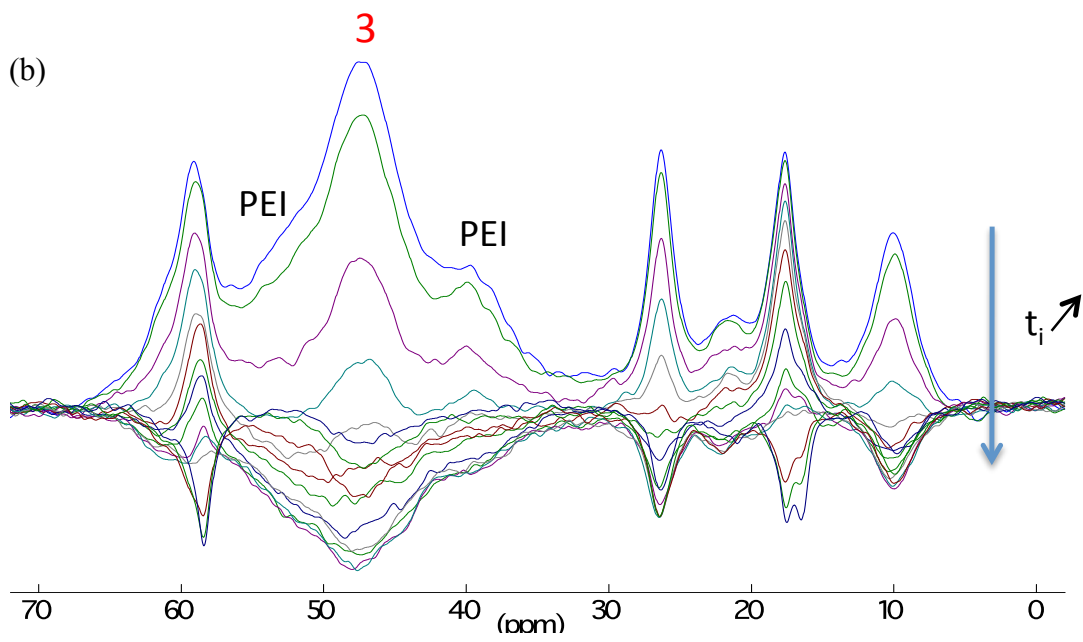


Figure S5. Viability of 3T3 fibroblast cells at the end of the transfection experiments, as determined by the Alamar Blue assay

